Crystal Structure and Crystal Chemistry of the τ-$Mg_{32}(Al,Zn)_{49}$ Solid Solution Using First-Principles Calculations and Thermodynamic modelling.

Minh Duc Vo[a], Paul Lafaye[a]*, Javier Jofre[a], Jean-Philippe Harvey[a]

[a] *CRCT- Polytechnique Montréal, Chem. Eng., Box 6079, Station Downtown, Montréal, Qc, Canada, H3C 3A7*

Abstract

This paper presents a study of the crystal structure and crystal chemistry of the τ-$Mg_{32}(Al,Zn)_{49}$ phase. We first performed DFT calculations to resolve conflicting data concerning the occupancy of site 2*a* of the solid solution crystal structure. Subsequently, 16 ordered configurations derived from the mixing of Al/Zn on sites $24g_1$, $24g_2$ and 48*h* of the solid solution structure, as well as the mixing of Mg/Zn on site $12e_1$ were generated. We then used DFT calculations to derive the formation enthalpies of all the *end-members* of the solid solution, their elastic constants by imposing 51 finite deformations for each *end-member*, and their energies as a function of volume. These calculations were used in a Debye-Wang model (in Slater form) to calculate the heat capacities of the 16 *end-members* and to obtain *in fine* their Gibbs energies. At last, these calculations were used to support a thermodynamic model based on the Bragg-Williams approximation, enabling all mixed sites occupancies to be calculated at any temperature and chemical composition. For instance, the predictions we carried out at 633 K and 800 K are in very good agreement with the available measurements. On the basis of these new results, we have determined the chemical ordering of the solid solution over a very wide range of chemical composition and temperature, which has enabled us to propose a new sublattice model for the τ-$Mg_{32}(Al,Zn)_{49}$ solid solution. This sublattice model is both simpler and more accurate than all the other models used in the literature since it agrees with the crystal structure and the crystal chemistry of the τ-$Mg_{32}(Al,Zn)_{49}$ phase in a large range of temperature and chemical composition.

---

*Corresponding author
E-mail address: paul.lafaye@polymtl.ca

Introduction

There is a large interest in the development of new magnesium alloys containing a wide range of alloying elements (especially rare earth elements) for the aerospace and transportation industries due to their high specific strength compared to other materials [1, 2]. In the automotive industry, the potential use of magnesium alloys for various components such as cradles and body sheets in the future could yield noticeable weight savings compared to traditional aluminum alloys [3, 4]. The limited strength and low room temperature ductility of Mg alloys are the main limiting factors that actually prevent their integration in the industrial production chain of high performance components [1, 2]. The development of new magnesium alloys with improved mechanical properties requires the screening of a virtually infinite chemical space in which alloying elements can be added to promote the formation of various precipitates in the HCP Mg matrix. [5, 6]. Aluminum and zinc are common elements added to magnesium alloys; they are the main alloying elements present in the AZ and ZA series of magnesium alloys [7, 8]. The addition of these elements in magnesium alloys leads to the formation of important strengthening phases at the grain boundaries such as β-$Mg_{17}Al_{12}$, $MgZn_2$, Φ-$Mg_5Al_2Zn_2$ and τ-$Mg_{32}(Al,Zn)_{49}$ [9, 10]. As these precipitates improve the strength of magnesium alloys and their formation is desired, it is necessary to be able to precisely predict their thermodynamic stability during alloy design [11-13].

The Calphad method [14] plays a central role in the Integrated Computational Materials Engineering used to develop the next generation of alloys. It allows the prediction of phase equilibria as well as the precipitation sequence of phases under both equilibrium cooling and infinitely fast cooling (also called Scheil cooling). The effectiveness of the CALPHAD method relies on the accuracy of the thermodynamic models used to describe the energetics of both stable and metastable phases. For solid solutions, the construction of an optimal sublattice model which is consistent with their crystal structure ensures the optimal fitting of the available experimental data coupled to good interpolations/extrapolation behaviors. The definition of the optimal sublattice model is particularly critical when dealing with the τ-$Mg_{32}(Al,Zn)_{49}$ phase because it exhibits a relatively large homogeneity range in the Mg-Al-Zn ternary system [15]. Although the frequently used stoichiometric formula $Mg_{32}(Al,Zn)_{49}$ [15] suggests a semi-stoichiometric compound with fixed magnesium composition, its concentration varies from 32 to 45 at.% [15]. For zinc, the nominal composition ranges from about 15 to 50 at.%. These evidences strongly suggest the need to describe the τ-$Mg_{32}(Al,Zn)_{49}$ phase as a solid solution. Although the label τ-$Mg_{32}(Al,Zn)_{49}$ is unsuitable for describing the correct stoichiometry of this solid solution, we retained it throughout this article since it is by far the most commonly used name in the literature. The existing sublattice models of the τ-$Mg_{32}(Al,Zn)_{49}$ phase available in the literature [15-18] are all based on the occupation of site 2*a*, as studied by Bergman *et al.* [19, 20]. Indeed, Bergman [19] proposed a crystallographic model of the τ-$Mg_{32}(Al,Zn)_{49}$

phase comprising eight crystal sites: site 2*a* occupied by Al; sites 12e_1, 12e_2, 16*f*, and 24g_3 occupied by Mg; and sites 24g_1, 24g_2, and 48*h* as mixed Al/Zn sites. However, more recent studies have suggested that the site 2*a* is in fact vacant [21, 22]. Since the crystal structure of the solid solution has not been definitely established, these thermodynamic models potentially perpetuate an erroneous description of the τ-$Mg_{32}(Al,Zn)_{49}$ solid solution. In addition, all the sublattice models proposed in the literature are based on assumptions made to adequately reproduce the homogeneity range of the τ-$Mg_{32}(Al,Zn)_{49}$ phase. Although these assumptions do not necessarily lack merit, such sublattice models can only lead to an erroneous description of the thermodynamic stability of the solid solution due to an incorrect description of its configurational entropy of mixing, leading to interpolation/extrapolation problems for higher order systems [23-26].

The motivation for this work is first to clarify the crystal structure of the solid solution and also to propose a new and accurate sublattice model for the τ-$Mg_{32}(Al,Zn)_{49}$ solid solution. To this end, characterization of the crystal chemistry and the quantification of the chemical ordering of the solid solution was performed using first-principles calculations and thermodynamic modelling. Indeed, the enthalpies of formation, elastic constants, and heat capacities of all the ordered configurations resulting from substitution of Al/Zn on sites 24g_1, 24g_2 and 48*h* and substitution of Mg/Zn on site 12e_1 of the structure of the τ-$Mg_{32}(Al,Zn)_{49}$ phase were calculated using Density Functional Theory (DFT). The site occupation factors (*sof*) were then computed at different temperatures based on the Compound Energy Formalism (CEF) [14], simulating the complete substitution of each element on the crystal sites. These new data were used to quantify the chemical ordering of the solid solution in the Mg-Al-Zn ternary system and finally to propose a new sublattice model. As discussed in this paper, the resulting sublattice model is more reliable and constructed with a foundation consistent with the crystal chemistry and crystal structure of the τ-$Mg_{32}(Al,Zn)_{49}$ phase.

Literature review

In the first complete investigation of the ternary Mg-Al-Zn system, Eger [27] published a liquidus projection and several temperature-composition isopleth sections for this system which established the presence of two ternary solid phases. Subsequent investigations of the ternary system confirmed the presence of such ternary phases, which were identified as the φ phase with $Al_2Mg_5Zn_2$ stoichiometric formula and τ (or T) phase with $Al_2Mg_3Zn_3$ or $Al_6Mg_{11}Zn_{11}$ stoichiometric formula [28]. The latter τ-$Mg_{32}(Al,Zn)_{49}$ phase is important for the description of AZ and ZA magnesium alloys [7-10] as well as for the study of the 7000 series aluminum alloys. It is a strengthening precipitate for these alloys and its formation has been the subject of many experimental and theoretical studies [29-35].

The crystal structure of the τ phase was initially identified through XRD studies by Laves *et al.* [36] as a body-centred cubic with a = 14.16 Å and with 161 atoms per unit cubic cell. Laves *et al.* [36] , at the time, also noted similarities between this Mg-Al-Zn phase and a ternary phase of the Mg-Al-Cu system with approximate composition Mg_4Al_6Cu. More recent XRD investigations carried out by Bergman *et al.* [19, 20] refined the description of the crystal structure; they confirmed a cubic structure with space group *Im*3 (204). However, the estimated total atoms per unit cell was increased to 162 with the idealized formula $Mg_{32}(Al,Zn)_{49}$. Of note, a central site 2*a* partially occupied by aluminum was identified by Bergman *et al.* [19]. The crystallography of the τ phase as described by Bergman *et al.* [19] is presented in Table 1.

Table 1. Crystal structure of the τ-$Mg_{32}(Al,Zn)_{49}$ phase as described by Bergman *et al.* [19].

Wyckoff position	Occupancy	Coordination	x	y	z
2*a*	(80%) Al	12	0	0	0
$24g_1$	81% Zn / 19% Al	12	0	0.0908	0.1501
$24g_2$	57% Zn / 43% Al	12	0	0.1748	0.3007
16*f*	100 % Mg	16	0.1836	0	0
$24g_3$	100 % Mg	16	0	0.2942	0.1194
48*h*	64% Zn / 36% Al	12	0.1680	0.1860	0.4031
$12e_1$	100 % Mg	14	0.4002	0	0
$12e_2$	100 % Mg	15	0.1797	0	0

Single crystal XRD studies by Sun *et al.* [21] evaluated the impact of zinc concentration on the crystal structure of the τ-$Mg_{32}(Al,Zn)_{49}$ phase. These authors measured the zinc *sof* in samples with content of Zn varying from 14 to 51 at.%. They also found a preferential insertion of zinc on site $24g_1$. Notably, Sun et al. [21] found a zinc occupation of 0.12 on site $12e_1$ even though this site remains fully occupied by Mg atoms for alloys containing 51 at.% Zn. In contrast to Bergman *et al.* [19], Sun *et al.* [21] found that no atoms were present on site 2*a* in any of the samples. Sun *et al.* [21] therefore proposed that site 2*a* is vacant throughout the entire composition range. More recently, Montagné *et al.* [22] studied the τ-$Mg_{32}(Al,Zn)_{49}$ phase with the nominal composition $Al_{12}Mg_{32}Zn_{37}$. In line with results from Sun *et al.* [21], Montagné *et al.* [22] identified substitution of Zn on site $12e_1$ and confirmed a vacancy at the central site 2*a*. *Sof* on sites $24g_1$, $24g_2$ and 48*h* are also in agreement with findings by Bergman *et al.* [19] and Sun *et al.* [21]. The *sof* found by Montagné *et al.* [22] at 633 K and 39.6 at.% Mg composition are presented in Table 2.

Table 2. Crystal structure of the τ-$Mg_{32}(Al,Zn)_{49}$ phase, occupancy from Montagné *et al.* [22].

Sites	Wyckoff position	Occupancy	Coordination	x	y	z
Mg (1)	$12e_1$	94.1% Mg / 5.9% Zn	14	0.4023	0	0.5000
Mg (2)	$12e_2$	100 % Mg	15	0.1981	0	0.5000
Mg (3)	16*f*	100 % Mg	16	0.1861	0.1861	0.1861
Mg (4)	$24g_3$	100 % Mg	16	0	0.3006	0.1163
Zn (1)	$24g_1$	87.3% Zn / 12.7% Al	12	0	0.0929	0.1512
Zn (2)	$24g_2$	72.2% Zn / 27.8% Al	12	0	0.1803	0.3066
Zn (3)	48*h*	71.9% Zn / 28.1% Al	12	0.1574	0.1916	0.4035
-	2*a*	(Vacant)	12	0	0	0

In a thermodynamic assessment of the Mg-Al-Zn ternary system, Liang H. *et al.* [37] used the formula $Mg_{32}(Al,Zn)_{49}$ proposed by Bergman *et al.* [19]. This idealized formula implies a semi-stoichiometric phase with a Mg composition around 39.5 at.% despite the phase diagram data indicating a wide homogeneity range of Mg going from 32 to 45 at.% Mg. Moreover, Liang P. *et al.* [15] performed EMPA measurements and found that the idealized formula $Mg_{32}(Al,Zn)_{49}$ could not properly model the homogeneity domain of the phase. Based on the crystallographic studies of Bergman *et al.* [19], Liang P. *et al.* [15] proposed that aluminum could be substituted with magnesium on site Mg (1) due to the lower ligancy compared to the other Mg sites. The resulting model is $(Mg)_{26}(Mg,Al)_6(Al,Zn,Mg)_{48}(Al)_1$. Liang P. *et al.* [15] also assumed that Cu could substitute in the third sublattice in order to reproduce the homogeneity range of the τ-$Mg_{32}(Al,Zn)_{49}$ phase in the Al-Cu-Mg-Zn quaternary system. The model proposed by Liang P. *et al.* [15] or variations of it have been reused in more recent assessments involving the Mg-Al-Zn system [16-18].

Methodology

DFT calculations

DFT calculations were performed using the VASP code [38, 39] with the Perdew-Burke-Ernzerhof exchange-correlation function [40] in the framework of the generalized gradient approximation using a 9×9×9 k-points grid and a cutoff energy of 600 eV. Projector augmented wave pseudopotentials with 3, 2 and 12 valence electrons were used for Al, Mg and Zn respectively. 16 *end-members* were considered based on the distribution of aluminum and zinc elements on sites $24g_1$, $24g_2$ and 48*h* and of magnesium and zinc

on site 12e_1. According to the most recent studies [21-22], site 2*a* is considered vacant, resulting in a total of 160 atoms per unit cell. The enthalpy of formation of the *end-members* is the difference between the calculated total energy and the sum of the pure element energies in their standard states (Al-*fcc*, Mg-*hcp*, Zn-*hcp*).

Debye model of the heat capacity calculations

The heat capacities were calculated using a Debye approach within the quasi-harmonic approximation [41]. The internal energy was parametrised by fitting the Birch-Murnaghan equation of state to the DFT total energy as function of volume calculated using the VASP code [38, 39]. The Slater form of the Debye-Wang model [42] was used to calculate the Debye temperature. The elastic constants of all *end-members* were calculated from the stress-strain tensor by imposing 51 finite distortions on the lattice and are reported in Table 4. The electronic contribution to the free energy was described as a function of the volume-dependent electronic density of state evaluated at the Fermi level. The calculated heat capacities for the 16 *end-members* are presented in Table 5.

Thermodynamic modelling

Using the Compound Energy Formalism (CEF) [14], the Gibbs free energy of the solution is evaluated at finite temperature from the calculations of the formation enthalpy and isobaric heat capacity of all the solution *end-members*. The configuration entropy is based on the Bragg-Williams model, considering only ideal mixing on each sublattice (i.e. without adding other non-ideal excess energy contributions). Additional information on the formalism is readily available in the literature including previous work using this methodology [43, 44].

Results and discussion

In this work, we first performed DFT calculations to elucidate the occupancy of site 2*a* in the solid solution structure, addressing discrepancies in existing crystallographic data. Initially, the mixed sites of the structure were considered as fully occupied by the predominant element according to Montagné *et al.* [22] (site 12e_1 occupied by Mg, sites 24g_1, 24g_2 and 48*h* occupied by Zn), while site 2*a* was successively considered as vacant, 50% occupied by Al and then fully occupied by Al. The enthalpies of formation

calculated by DFT give -12.223 kJ/mol-at for vacant site 2*a*, compared with -11.674 kJ/mol-at and -11.944 kJ/mol-at for alternative occupancy scenarios. We also carried out additional calculations, based on the measurements performed by Montagné *et al.* [22], to explore potential Al occupancy on sites $24g_2$ and 48*h*, while maintaining the occupancy of Mg on site $12e_1$ and Zn on site $24g_1$. The DFT calculations revealed enthalpies of formation of -5.274 kJ/mol-at for vacant site 2*a*, contrasting with -4.327 kJ/mol-at and -4.687 kJ/mol-at for the other two structures. Based on our analyses, we ascertain that site 2*a* within the crystal structure of the τ-$Mg_{32}(Al,Zn)_{49}$ solid solution is vacant, corroborating recent literature data [21, 22]. Consequently, the notation established in Table 2 will be consistently employed throughout this paper.

The calculated total energies and formation enthalpies at 0 K for the 16 configurations are reported in Table 3.

Table 3. DFT calculated total energy (E_{tot}) and enthalpy of formation (ΔH_f) of the τ-$Mg_{32}(Al,Zn)_{49}$ solid solution *end-members*. Reference Al (*fcc*), Mg (*hcp*) and Zn (*hcp*).

Mg (1) 12	Mg (2-4) 52	Zn (1) 24	Zn (2) 24	Zn (3) 48	E_{tot} (eV)	ΔH_f (kJ/mol)
Zn	Mg	Al	Al	Al	-452.554	-0.772
Mg	Mg	Al	Al	Al	-458.932	-1.736
Zn	Mg	Al	Zn	Al	-394.576	-4.002
Mg	Mg	Al	Zn	Al	-400.924	-4.947
Zn	Mg	Zn	Al	Al	-395.204	-4.381
Mg	Mg	Zn	Al	Al	-401.466	-5.274
Zn	Mg	Al	Al	Zn	-335.353	-6.481
Mg	Mg	Al	Al	Zn	-341.030	-7.021
Zn	Mg	Zn	Zn	Al	-337.386	-7.707
Mg	Mg	Zn	Zn	Al	-342.994	-8.206
Zn	Mg	Al	Zn	Zn	-276.453	-9.154
Mg	Mg	Al	Zn	Zn	-281.326	-9.210
Zn	Mg	Zn	Al	Zn	-279.741	-11.137
Mg	Mg	Zn	Al	Zn	-284.402	-11.065
Zn	Mg	Zn	Zn	Zn	-218.580	-12.447
Mg	Mg	Zn	Zn	Zn	-222.988	-12.223

The comparison between our calculations and those of Song *et al.* [45] is limited since these authors only considered two chemical compositions for the τ-$Mg_{32}(Al,Zn)_{49}$ phase with an erroneous crystal structure [22]. The *end-members* they studied with compositions $Al_{26}Zn_{72}Mg_{64}$ and $Al_{50}Zn_{48}Mg_{64}$ have enthalpies of formation of -9.728 kJ/mol-at (vs -11.137 kJ/mol-at in this work) and -6.952 kJ/mol-at (vs -8.206 kJ/mol-

at in this work), respectively. These results are again consistent with recent crystallographic studies suggesting that site 2*a* is not occupied.

From these DFT calculations, it was possible to determine the enthalpy of mixing at 0 K of the τ-$Mg_{32}(Al,Zn)_{49}$ solid solution using the binary configurations as reference states. Figure 1 presents the enthalpy of mixing for the solid solution for 40 at. % Mg.

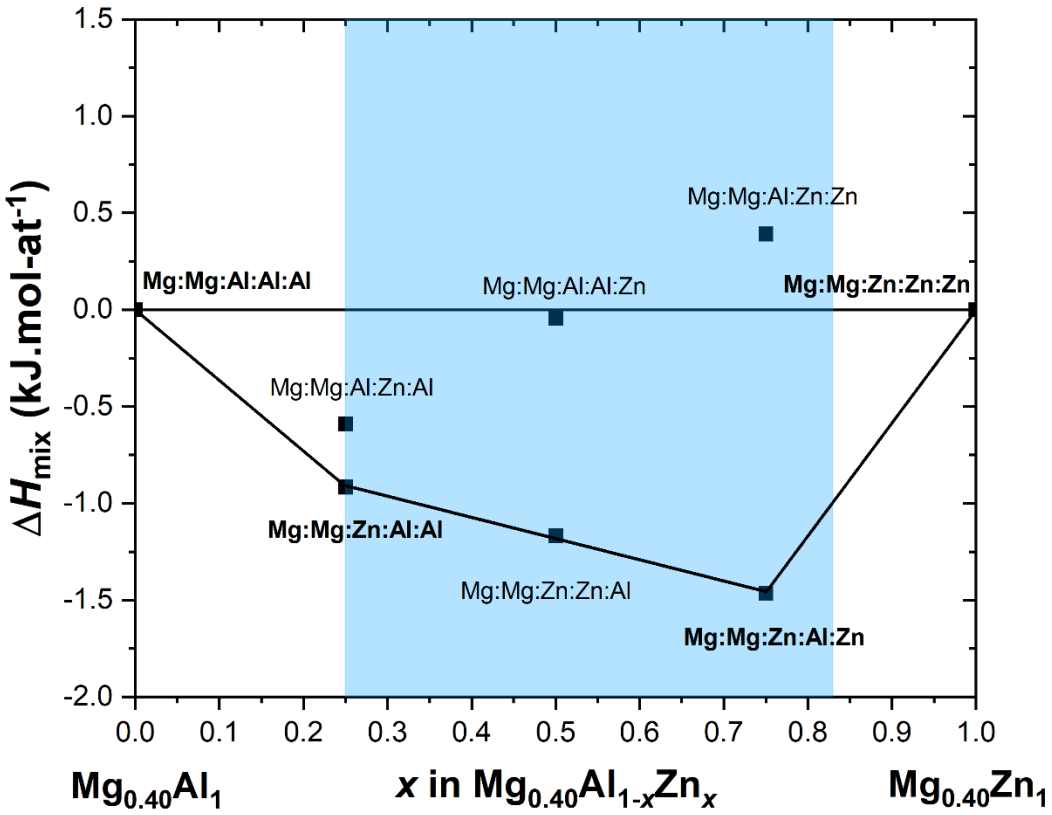

Figure 1. Mixing enthalpy of the τ-$Mg_{32}(Al,Zn)_{49}$ solid solution at a composition of 40 at.% Mg calculated at 0 K. The reported homogeneity range of the phase is highlighted by the blue band. References are $Al_1Mg_{0.40}$ and $Zn_1Mg_{0.40}$. *End-members* are identified according to the notation Mg(1):Mg(2-4):Zn(1):Zn(2):Zn(3). *End-members* in bold are stable at 0 K.

The mixing enthalpy curve presented in Figure 1 indicates a progressive and sequential substitution of zinc on the Zn sites at 0 K. Indeed, the preferential order for zinc substitution is Zn (1) > Zn (3) > Zn (2). The *ground state* at 0 K includes the *end-members* Mg:Mg:Al:Al:Al, Mg:Mg:Zn:Al:Al, Mg:Mg:Zn:Al:Zn and

Mg:Mg:Zn:Zn:Zn. It is interesting to note that the *end-member* Mg:Mg:Zn:Zn:Al is very close to the *ground state*, revealing that sites Zn (3) and Zn (2) are almost equivalent for Zn substitution around the composition $x = 0.5$ in this $Mg_{0.40}Al_{1-x}Zn_x$ section. It also should be noted that zinc substitution on site Zn (3) is favored when site Zn (1) is substituted by zinc. Note that from these calculations, the chemical ordering of the solution appears relatively weak since the mixing enthalpy does not exceed a few kJ per mol-at. for all *end-members*. The calculated elastic constants of the *end-members* of the τ-$Mg_{32}(Al,Zn)_{49}$ are presented in Table 4.

Table 4. Calculated elastic constants of the τ-$Mg_{32}(Al,Zn)_{49}$ solid solution *end-members*. Reference Al (*fcc*), Mg (*hcp*) and Zn (*hcp*).

Mg (1)	Mg (2-4)	Zn (1)	Zn (2)	Zn (3)	Elastic constants (GPa)		
12	52	24	24	48	C_{11}	C_{12}	C_{44}
Zn	Mg	Al	Al	Al	89.5	44.3	19.7
Mg	Mg	Al	Al	Al	89.0	42.2	20.0
Zn	Mg	Al	Zn	Al	93.0	46.9	22.1
Mg	Mg	Al	Zn	Al	97.0	40.5	23.4
Mg	Mg	Zn	Al	Al	97.4	39.9	24.6
Zn	Mg	Zn	Al	Al	92.6	45.8	23.2
Zn	Mg	Al	Al	Zn	103.7	39.8	25.7
Mg	Mg	Al	Al	Zn	103.5	37.1	27.0
Zn	Mg	Zn	Zn	Al	106.8	43.1	31.4
Mg	Mg	Zn	Zn	Al	103.7	37.6	31.0
Zn	Mg	Al	Zn	Zn	107.2	37.1	31.2
Mg	Mg	Al	Zn	Zn	102.2	36.7	29.3
Zn	Mg	Zn	Al	Zn	117.3	39.4	37.6
Mg	Mg	Zn	Al	Zn	109.0	39.1	35.3
Zn	Mg	Zn	Zn	Zn	111.8	42.9	35.6
Mg	Mg	Zn	Zn	Zn	101.0	40.1	32.8

As with the DFT calculations of the formation enthalpies of the solid solution end-members, our calculations of the elastic constants cannot be compared with those available in the literature [45], since they were based on the crystal structure determined by Bergman *et al.* [19], although this proved to be erroneous [22].

The elastic constants were used along with a Debye-Wang model (in Slater form) to calculate the heat capacities of the *end-members* of the τ-$Mg_{32}(Al,Zn)_{49}$ solid solution. The results are presented in Table 5.

Table 5. Calculated heat capacities of the τ-$Mg_{32}(Al,Zn)_{49}$ solid solution *end-members*. Reference Al (*fcc*), Mg (*hcp*) and Zn (*hcp*).

Mg (1)	Mg (2-4)	Zn (1)	Zn (2)	Zn (3)	Heat capacity, Cp (J/K.mol-at.)					
12	52	24	24	48	10^{1}	10^{-3} T	10^{5} T^{-2}	10^{-7} T^{2}	10^{1} $T^{-0.5}$	10^{7} T^{-3}
Zn	Mg	Al	Al	Al	2.427	3.731	-0.241	-4.059	1.145	0.188
Mg	Mg	Al	Al	Al	2.445	3.424	-0.194	-3.484	0.835	0.130
Zn	Mg	Al	Zn	Al	2.414	4.039	-0.268	-4.710	1.367	0.223
Mg	Mg	Al	Zn	Al	2.413	3.983	-0.292	-4.628	1.399	0.239
Mg	Mg	Zn	Al	Al	2.424	3.863	-0.241	-4.330	1.174	0.173
Zn	Mg	Zn	Al	Al	2.414	3.993	-0.270	-4.604	1.363	0.221
Zn	Mg	Al	Al	Zn	2.384	4.536	-0.358	-5.845	1.882	0.310
Mg	Mg	Al	Al	Zn	2.403	4.256	-0.297	-5.287	1.536	0.235
Zn	Mg	Zn	Zn	Al	2.393	4.356	-0.322	-5.387	1.702	0.263
Mg	Mg	Zn	Zn	Al	2.402	4.139	-0.327	-4.988	1.585	0.271
Zn	Mg	Al	Zn	Zn	2.352	4.994	-0.449	-6.940	2.425	0.401
Mg	Mg	Al	Zn	Zn	2.378	4.720	-0.355	-6.375	1.959	0.293
Zn	Mg	Zn	Al	Zn	2.352	4.938	-0.452	-6.737	2.425	0.397
Mg	Mg	Zn	Al	Zn	2.370	4.682	-0.401	-6.264	2.113	0.346
Zn	Mg	Zn	Zn	Zn	2.326	5.420	-0.510	-8.009	2.864	0.462
Mg	Mg	Zn	Zn	Zn	2.374	5.090	-0.314	-7.201	1.942	0.242

As no measure of the heat capacity was available in the literature for these crystal structures, the calculations performed in this work are from this perspective an important contribution for the thermodynamic description of the phase. From the DFT calculations reported in Table 3 and the calculated heat capacities reported in Table 5, the zinc *sof* on the various sites were computed 633 K and 800 K for a composition of 40 at. % Mg as presented in Figures 2 and 3.

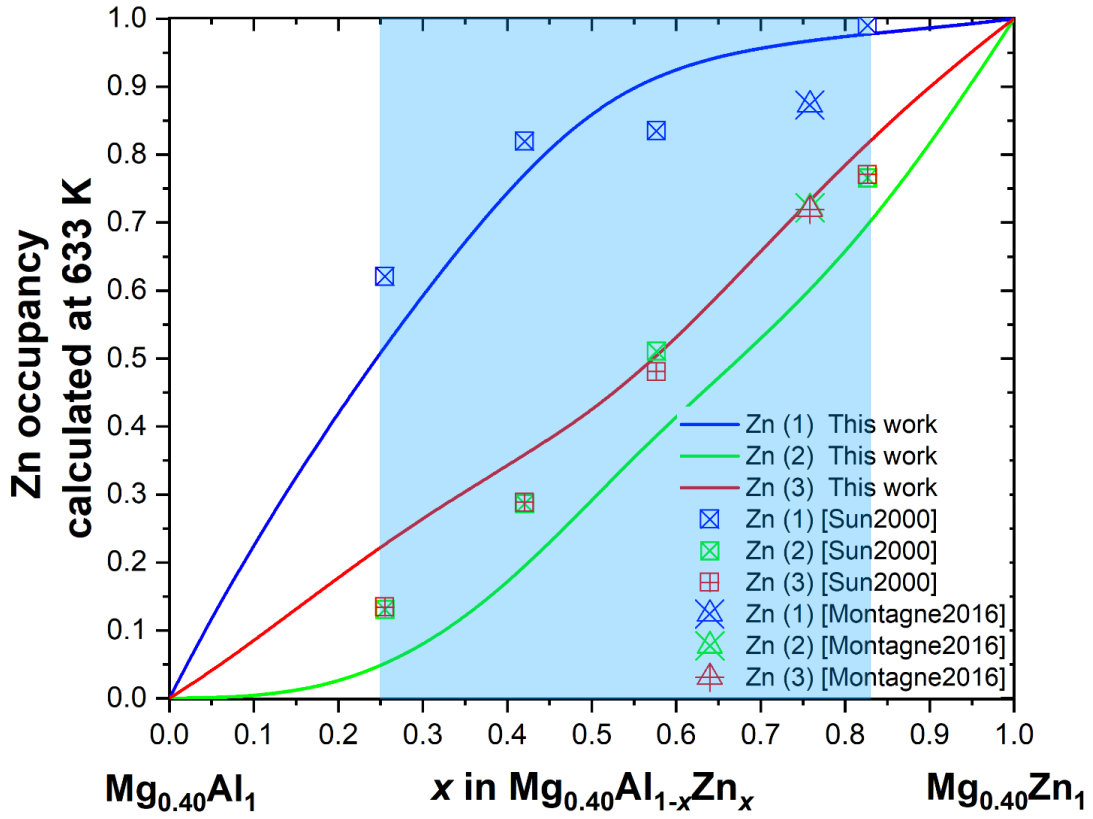

Figure 2. Zn site occupation factors in the τ-$Mg_{32}(Al,Zn)_{49}$ solid solution at a composition of 40 at.% Mg calculated at 633 K. The reported homogeneity range of the phase is highlighted by the blue band. References are $Al_1Mg_{0.40}$ and $Zn_1Mg_{0.40}$. * Montagné *et al.* [22] and Sun *et al.* [21] carried out measurements on alloys containing 39.5 at.% Mg. The chemical compositions studied in this paper (40 at.% Mg) are considered reasonably close for a meaningful comparison.

First of all, let's note the remarkable accuracy of our *ab-initio*-based thermodynamic model for predicting the *sof*. Indeed, the calculated *sof* are in good agreement with measurements reported in the literature at 633 K and 800 K. The preferred order for zinc substitution is found to be Zn (1) > Zn (3) > Zn (2) which is consistent with our previous conclusions from Figure 1. According to our calculations and literature data, preference for site Zn (1) is much stronger compared to sites Zn (3) and Zn (2). Indeed, experimental studies by Sun *et al.* [21] and Montagné *et al.* [22] gave near identical zinc occupation for Zn (2) and Zn (3) which is also in line with our previous findings from Figure 1. On the other hand, our calculations reveal a slight

preference for site Zn (3) over site Zn (2) which is experimentally observed at 800 K but not evidenced at 633 K.

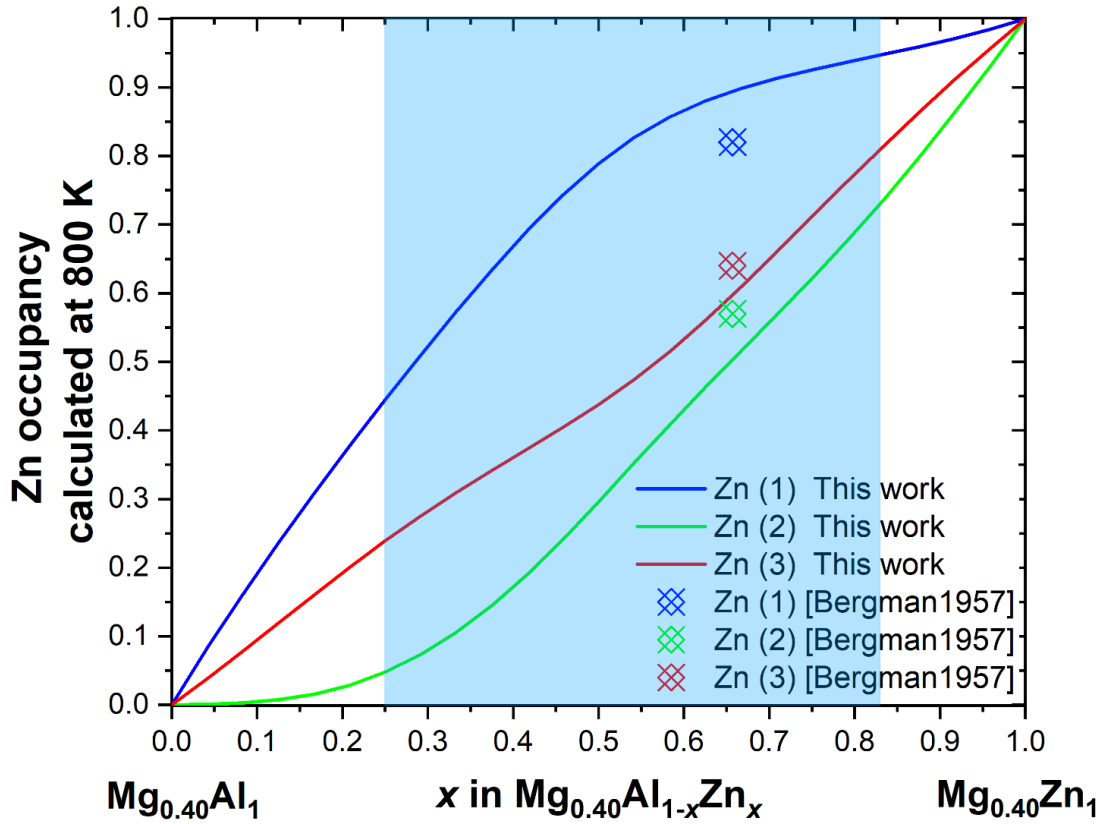

Figure 3. Zn site occupation factors in the τ-$Mg_{32}(Al,Zn)_{49}$ solid solution at a composition of 40 at.% Mg calculated at 800 K. The reported homogeneity range of the phase is highlighted by the blue region. References are $Al_1Mg_{0.40}$ and $Zn_1Mg_{0.40}$. * Montagné *et al.* [22] and Sun *et al.* [21] carried out measurements on alloys containing 39.5 at.% Mg. The chemical compositions studied in this paper (40 at.% Mg) are considered reasonably close for a meaningful comparison.

At 800 K, near the fusion temperature of the τ-$Mg_{32}(Al,Zn)_{49}$ phase, a reduction of the chemical ordering of the sites is observed since *sof* values approach the molar fraction of *x* in $Mg_{0.40}Al_{1-x}Zn_x$. Finally, it should be noted that our methodology for calculating *sof* assumes that there is no short-range ordering within the solid solution. The good agreement between our calculations and *sof* measurements validates this assumption as well as our DFT calculations for both formation enthalpy and heat capacity. Additionally, to

our knowledge, it is worth noting that no direct calculations of short-range ordering have been carried out for this phase.

In the perspective of proposing a sublattice model for the τ-$Mg_{32}(Al,Zn)_{49}$ phase, the chemical ordering of the Zn sites can be better quantified through the configurational entropy of mixing. As such, the configurational entropy of mixing of the τ-$Mg_{32}(Al,Zn)_{49}$ solid solution at a composition of 40 at.% Mg was calculated using the *sof* obtained previously and are presented in Figures 4 and 5.

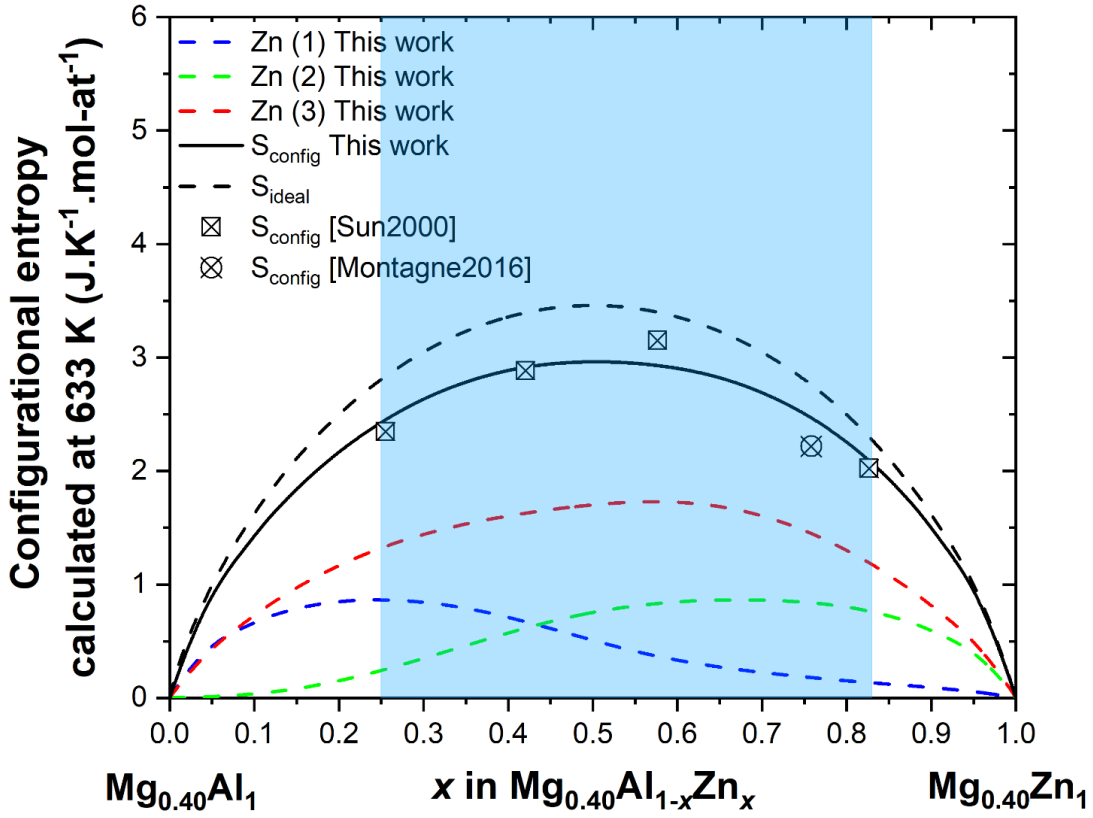

Figure 4. Configuration entropy of mixing (refs.: $Al_1Mg_{0.40}$ and $Zn_1Mg_{0.40}$) of the τ-$Mg_{32}(Al,Zn)_{49}$ solid solution at a composition of 40 at.% Mg calculated at 633 K. The individual contribution of each site is represented by the colored dashed lines and the total configuration entropy is presented by the black line. The ideal configuration entropy of mixing is represented by the black dashed line. The reported homogeneity range of the phase is highlighted by the blue region. * Montagné *et al.* [22] and Sun *et al.* [21] carried out measurements on alloys containing 39.5 at.% Mg. The chemical compositions studied in this paper (40 at.% Mg) are considered reasonably close for a meaningful comparison.

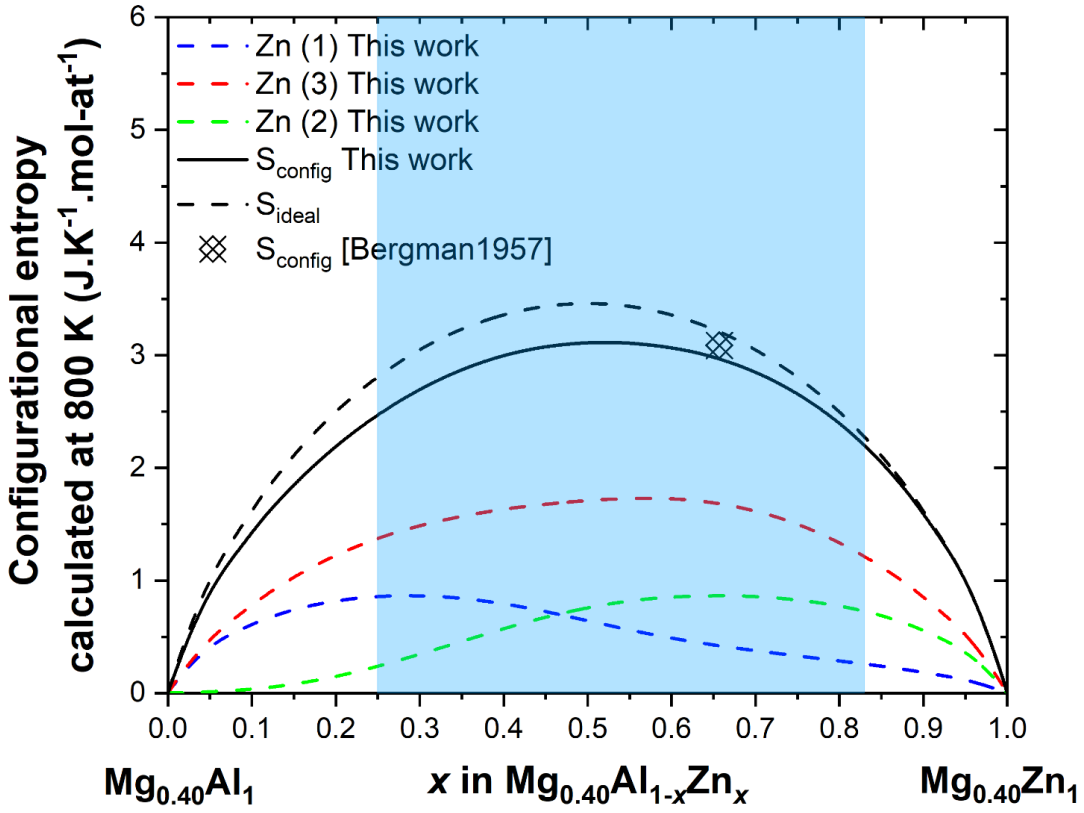

Figure 5. Configuration entropy of mixing (refs.: $Al_1Mg_{0.40}$ and $Zn_1Mg_{0.40}$) of the τ-$Mg_{32}(Al,Zn)_{49}$ solid solution at a composition of 40 at.% Mg calculated at 800 K. The individual contribution of each site is represented by the colored dashed lines and the total configuration entropy is indicated by the black line. The ideal configuration entropy of mixing is represented by the black dashed line. The reported homogeneity range of the phase is highlighted by the blue region. * Montagné *et al.* [22] and Sun *et al.* [21] carried out measurements on alloys containing 39.5 at.% Mg. The chemical compositions studied in this paper (40 at.% Mg) are considered reasonably close for a meaningful comparison.

At temperatures of 633 K and 800 K, the calculated configurational entropy of mixing is close to the ideal mixing behavior. The values calculated in this work are in good agreement with results from Bergman *et al.* [20], Sun *et al.* [21] and Montagné *et al.* [22]. Considering the results of these calculations, the chemical ordering of zinc on the Zn sites of the τ-$Mg_{32}(Al,Zn)_{49}$ phase structure appears relatively weak and in agreement to our qualitative inference from mixing enthalpy curves. The combination of sites Zn (1), Zn (2) and Zn (3) in a single sublattice is therefore recommended.

The τ-$Mg_{32}(Al,Zn)_{49}$ homogeneity range is predominantly around a composition of 40 at.% Mg. Zinc substitution on the Mg (1) allows for compositions below 40 at.% Mg which was observed in experimental studies by Sun *et al.* [21] and Montagné *et al.* [22]. Thermodynamic models [15-18] used to describe the τ-$Mg_{32}(Al,Zn)_{49}$ phase proposed an aluminum substitution but this was not observed by Sun *et al.* [21] or Montagné *et al.* [22]. For compositions above 40 at.% Mg, a substitution of magnesium in one or all sites Zn (1), Zn (2) and/or Zn (3) was proposed in thermodynamic assessments of the τ-$Mg_{32}(Al,Zn)_{49}$ phase [15-18]. As our model groups all Zn sites into a single sublattice, the homogeneity range of the τ-$Mg_{32}(Al,Zn)_{49}$ phase above 40 at. % Mg will necessarily assume ideal magnesium substitution on sites Zn (1), Zn (2) and Zn (3). This model is valid since the Mg sites of the structure show maximum ordering at 40 at. % Mg and the homogeneity range of the solution extends only slightly beyond this. As a result, the substitution of Mg on the Zn sites will have only a marginal impact on the configurational entropy of the solution. Therefore, it was not considered critical to perform calculations for magnesium substitution on Zn sites for this work. The Gibbs free energy functions for the *end-members* of the proposed sublattice model for the τ-$Mg_{32}(Al,Zn)_{49}$ solid solution are presented in Table 6.

Table 6. Gibbs free energy of the τ-$Mg_{32}(Al,Zn)_{49}$ solid solution *end-members* according to the three sublattice model developed in this study. Reference Al (*fcc*), Mg (*hcp*) and Zn (*hcp*).

Sublattice			Parameters (J/mol-at.)
SL 1	SL 2	SL 3	
Multiplicity			
12	52	96	
Zn	Mg	Al	$-1.285\times10^{6}+2.206\times10^{4}\times T-3.997\times10^{3}\times T\times\ln(T)$ $-3.327\times10^{-1}\times T^{2}-2.06699\times10^{-5}\times T^{3}+5.041\times10^{5}\times T^{-1}$
Mg	Mg	Al	$-1.437\times10^{6}+2.215\times10^{4}\times T-3.995\times10^{3}\times T\times\ln(T)$ $-3.198\times10^{-1}\times T^{2}-1.7280\times10^{-5}\times T^{3}+5.452\times10^{5}\times T^{-1}$
Zn	Mg	Zn	$-3.183\times10^{6}+2.091\times10^{4}\times T-4.010\times10^{3}\times T\times\ln(T)$ $-3.904\times10^{-1}\times T^{2}-4.4919\times10^{-5}\times T^{3}+5.942\times10^{5}\times T^{-1}$
Mg	Mg	Zn	$-3.192\times10^{6}+2.101\times10^{4}\times T-4.008\times10^{3}\times T\times\ln(T)$ $-3.921\times10^{-1}\times T^{2}-4.2601\times10^{-5}\times T^{3}+5.783\times10^{5}\times T^{-1}$

The proposed model is therefore $(Mg,Zn)_{12}Mg_{52}(Al,Zn,Mg)_{96}$ or equivalent $(Mg,Zn)_{6}Mg_{26}(Al,Zn,Mg)_{48}$. Six *end-members* allow for the description of the whole homogeneity range of the τ-$Mg_{32}(Al,Zn)_{49}$ solid solution. Figure 6 presents the *end-members* for the model proposed in this work along with *end-members* for models used in the literature.

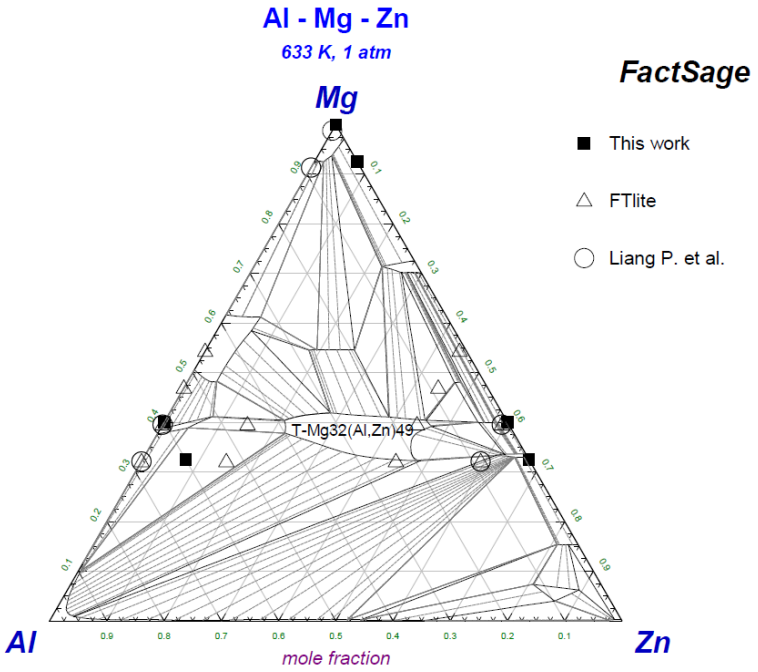

Figure 6. *End-members* of the sublattice model proposed in this work and other models of the τ-$Mg_{32}(Al,Zn)_{49}$ phase overlaid on the Mg-Al-Zn ternary system at 633 K according to the FTlite database of FactSage.

This model takes into consideration new crystallographic information [21, 22] for other sites and uses new DFT and heat capacity calculations for a more accurate representation of the crystal chemistry of the τ-$Mg_{32}(Al,Zn)_{49}$ phase. It also should be noted that the τ-$Mg_{32}(Al,Zn)_{49}$ solid solution follows the empirical rules governing the occupation of crystal sites in Frank-Kasper phases [46-47]. Magnesium, which has the largest atomic radius (160 pm), mainly occupies high coordination sites (15 and 16) which can accommodate its size. By contrast, aluminium (143 pm) and zinc (142 pm) preferentially occupy smaller, low-coordination sites (12), which have an electronic environment similar to that of *fcc* and *hcp* structures. It should be noted that the site with a coordination number of 14 can also be considered a high-coordination site, facilitating the occupation of magnesium while allowing limited occupation of zinc.

Conclusion

- The crystal structure of the τ-$Mg_{32}(Al,Zn)_{49}$ has been clarified, site 2*a* is vacant, in line with the most recent experimental data.
- All relevant substitutions of Al/Zn on sites 24g_1, 24g_2 and 48*h* and of Mg/Zn on 12e_1 based on crystallographic studies of the τ-$Mg_{32}(Al,Zn)_{49}$ phase found in the literature have been considered in this work. The enthalpy of formation, elastic constants, heat capacity and Gibbs energy of all 16 *end-members* were calculated using DFT calculations.
- A thermodynamic modelling of the τ-$Mg_{32}(Al,Zn)_{49}$ solid solution was proposed allowing the *sof* to be computed at different compositions and temperatures. These calculated *sof* are in good agreement with experimental *sof* of various authors at 633 K and 800 K. The level of chemical ordering was quantified at 633 K and 800 K from our *sof* calculations revealing the ideal nature of the solid solution.
- The new sublattice model of the τ-$Mg_{32}(Al,Zn)_{49}$ phase proposed in this work is consistent with both the crystal structure and the crystal chemistry of the solid solution. This was not the case for the legacy sublattice models which were based on erroneous crystal structure and on practical considerations. The proposed sublattice model is more robust but also more simple than the previous one and is therefore a significant improvement in the description of the τ-$Mg_{32}(Al,Zn)_{49}$ phase.

Acknowledgement

- This work was financially supported by the Professor Harvey Discovery Grant (RGPIN-2017-06168) (NSERC).
- Funding support was obtained through the Alliance Grant (ALLRP 560998 - 20).
- Compute Quebec and Compute Canada are thanked for supplying the intensive calculation tools.

References

[1] I. Polmear, Magnesium alloys and applications, Materials science and technology 10(1) (1994) 1-16.
[2] J. Song, J. She, D. Chen, F. Pan, Latest research advances on magnesium and magnesium alloys worldwide, Journal of Magnesium and Alloys 8(1) (2020) 1-41.
[3] W.J. Joost, P.E. Krajewski, Towards magnesium alloys for high-volume automotive applications, Scripta Materialia 128 (2017) 107-112.
[4] J. Weiler, A review of magnesium die-castings for closure applications, Journal of Magnesium and Alloys 7(2) (2019) 297-304.
[5] W. Neil, M. Forsyth, P.C. Howlett, C. Hutchinson, B.R.W. Hinton, Corrosion of magnesium alloy ZE41–The role of microstructural features, Corrosion science 51(2) (2009) 387-394.
[6] S.K. Baral, M.M. Thawre, B.R. Sunil, R. Dumpala, A review on developing high-performance ZE41 magnesium alloy by using bulk deformation and surface modification methods, Journal of Magnesium and Alloys (2023).
[7] F. Wang, T. Hu, Y. Zhang, W. Xiao, C. Ma, Effects of Al and Zn contents on the microstructure and mechanical properties of Mg-Al-Zn-Ca magnesium alloys, Materials Science and Engineering: A 704 (2017) 57-65.
[8] H. Feng, S. Liu, Y. Du, T. Lei, R. Zeng, T. Yuan, Effect of the second phases on corrosion behavior of the Mg-Al-Zn alloys, Journal of Alloys and Compounds 695 (2017) 2330-2338.
[9] S. Lv, Q. Yang, X. Lv, F. Meng, X. Qiu, Intermetallic phases and mechanical properties of a Mg–8Zn–6Al–1Sm (wt%) casting alloy, Materials Science and Engineering: A 852 (2022) 143719.
[10] S. Lv, Z. Xie, Q. Yang, F. Meng, X. Qiu, Microstructures and mechanical properties of a hot-extruded Mg− 8Zn− 6Al− 1Gd (wt%) alloy, Journal of Alloys and Compounds 904 (2022) 164040.
[11] Z.-Z. Shi, H.-T. Chen, K. Zhang, F.-Z. Dai, X.-F. Liu, Crystallography of precipitates in Mg alloys, Journal of Magnesium and Alloys 9(2) (2021) 416-431.
[12] K. Cheng, Y. Zheng, J. Sun, Y. Zhao, J. Wang, H. Yu, D. Zhao, H. Li, J. Zhou, Z. Ma, Investigation on the temperature-dependent diffusion growth of intermetallic compounds in the Mg-Al-Zn system: Experiment and modeling, Journal of Magnesium and Alloys (2023).
[13] X. Lv, L. Liu, Microstructure and mechanical performance of AZ31/6061 lap joints welded by laser-TIG hybrid welding with Zn-Al alloy filler metal, Journal of Magnesium and Alloys (2023).
[14] M. Hillert, The compound energy formalism, Journal of Alloys and Compounds 320(2) (2001) 161-176.
[15] P. Liang, T. Tarfa, J. Robinson, S. Wagner, P. Ochin, M. Harmelin, H. Seifert, H. Lukas, F. Aldinger, Experimental investigation and thermodynamic calculation of the Al–Mg–Zn system, Thermochimica Acta 314(1-2) (1998) 87-110.
[16] Q. Li, Y.-Z. Zhao, Q. Luo, S.-L. Chen, J.-Y. Zhang, K.-C. Chou, Experimental study and phase diagram calculation in Al–Zn–Mg–Si quaternary system, Journal of Alloys and Compounds 501(2) (2010) 282-290.
[17] Y. Du, S. Liu, L. Zhang, H. Xu, D. Zhao, A. Wang, L. Zhou, An overview on phase equilibria and thermodynamic modeling in multicomponent Al alloys: Focusing on the Al–Cu–Fe–Mg–Mn–Ni–Si–Zn system, Calphad 35(3) (2011) 427-445.
[18] Y. Yuan, F. Pan, D. Li, A. Watson, The re-assessment of the Mg–Zn and Fe–Si systems and their incorporation in thermodynamic descriptions of the Al–Mg–Zn and Fe–Si–Zn systems, Calphad 44 (2014) 54-61.
[19] G. Bergman, J.L. Waugh, L. Pauling, Crystal structure of the intermetallic compound Mg 32 (AI, Zn) 49 and related phases, Nature 169 (1952) 1057-1058.
[20] G. Bergman, J.L. Waugh, L. Pauling, The crystal structure of the metallic phase Mg32 (Al, Zn) 49, Acta Crystallographica 10(4) (1957) 254-259.
[21] W. Sun, F. Lincoln, K. Sugiyama, K. Hiraga, Structure refinement of (Al, Zn) 49Mg32-type phases by single-crystal X-ray diffraction, Materials Science and Engineering: A 294 (2000) 327-330.

[22] P. Montagné, M. Tillard, On the adaptability of 1/1 cubic approximant structure in the Mg–Al–Zn system with the particular example of Mg32Al12Zn37, Journal of Alloys and Compounds 656 (2016) 159-165.
[23] P. Lafaye, K. Oishi, M. Bourdon, J.-P. Harvey, Crystal chemistry and thermodynamic modelling of the Al13 (Fe, TM) 4 solid solutions (TM= Co, Cr, Ni, Pt), Journal of Alloys and Compounds 920 (2022) 165779.
[24] P. Lafaye, M.D. Vo, J.A. Jofre, J.-P. Harvey, Investigating the Al/Si Mixed Site Occupancy in the β-AlFeSi Phase, Physical Chemistry Chemical Physics (2023).
[25] P. Lafaye, K. Oishi, J.-P. Harvey, A comprehensive study on the thermodynamics of the Al13Fe4 solid solution in the Al-Fe-Mn ternary system, Journal of Alloys and Compounds 944 (2023) 169054.
[26] P. Lafaye, K. Poëti, J. Harvey, Ab-Initio Calculations, Debye-Wang Model and Thermodynamic Modeling for the Short-Range Order and Crystal Chemistry Characterization of the T8-Al2fe3si4 Solid Solution, Physica B: Condensed Matter 681 (2024) 415834.
[27] G. Eger, Studies on the constitution of the ternary Mg-Al-Zn alloys, Internationale Zeitschrift fur Metallographie 4 (1913) 50-128.
[28] P. Villars, Handbook of ternary alloy phase diagrams, ASM international 7 (1995) 8754-8755.
[29] L. Mondolfo, N. Gjostein, D. Levinson, Structural changes during the aging in an Al-Mg-Zn alloy, JOM 8 (1956) 1378-1385.
[30] C. Mondal, A. Mukhopadhyay, On the nature of T (Al2Mg3Zn3) and S (Al2CuMg) phases present in as-cast and annealed 7055 aluminum alloy, Materials Science and Engineering: A 391(1-2) (2005) 367-376.
[31] M. Suarez, O. Alvarez, M. Alvarez, R. Rodriguez, S. Valdez, J. Juarez, Characterization of microstructures obtained in wedge shaped Al–Zn–Mg ingots, Journal of Alloys and Compounds 492(1-2) (2010) 373-377.
[32] J. Yun, S. Kang, S. Lee, D. Bae, Development of heat-treatable Al-5Mg alloy sheets with the addition of Zn, Materials Science and Engineering: A 744 (2019) 21-27.
[33] S. Nakatsuka, M. Ishihara, N. Takata, A. Suzuki, M. Kobashi, Tensile properties of a heat-resistant aluminium alloy strengthened by T-Al6Mg11Zn11 intermetallic phase, MRS advances 4(25-26) (2019) 1485-1490.
[34] N. Takata, R. Takagi, R. Li, H. Ishii, A. Suzuki, M. Kobashi, Precipitation morphology and kinetics of T-Al6Mg11Zn11 intermetallic phase in Al–Mg–Zn ternary alloys, Intermetallics 139 (2021) 107364.
[35] Y. Geng, D. Zhang, J. Zhang, L. Zhuang, Early-stage clustering and precipitation behavior in the age-hardened Al–Mg–Zn (-Cu) alloys, Materials Science and Engineering: A 856 (2022) 144015.
[36] F. Laves, K. Löhberg, H. Witte, The Isomorphism of the Ternary Compounds Mg3Zn2Al2 and Mg4CuAl6, Metallwirtschaft 14 (1935) 793-794.
[37] H. Liang, S.-L. Chen, Y. Chang, A thermodynamic description of the Al-Mg-Zn system, Metallurgical and Materials Transactions A 28 (1997) 1725-1734.
[38] G. Kresse, J. Furthmüller, Efficient iterative schemes for ab initio total-energy calculations using a plane-wave basis set, Physical review B 54(16) (1996) 11169.
[39] G. Kresse, D. Joubert, From ultrasoft pseudopotentials to the projector augmented-wave method, Physical review b 59(3) (1999) 1758.
[40] J.P. Perdew, K. Burke, M. Ernzerhof, Generalized gradient approximation made simple, Physical review letters 77(18) (1996) 3865.
[41] M.A. Blanco, PhD Thesis, Universidad de Oviedo, 1997.
[42] Y. Wang, Z.-K. Liu, L.-Q. Chen, Thermodynamic properties of Al, Ni, NiAl, and Ni3Al from first-principles calculations, Acta Materialia 52(9) (2004) 2665-2671.
[43] P. Lafaye, Développement d'outils de modélisation thermodynamique pour la prédiction de l'état métallurgique d'alliages à base zirconium, Université Paris-Est, 2017.
[44] P. Lafaye, C. Toffolon-Masclet, J.-C. Crivello, J.-M. Joubert, Experimental study, first-principles calculation and thermodynamic modelling of the Cr–Fe–Nb–Sn–Zr quinary system for application as cladding materials in nuclear reactors, Journal of Nuclear Materials 544 (2021) 152692.

[45] Y. Song, S. Zhan, B. Nie, H. Qi, F. Liu, T. Fan, D. Chen, First-Principles Investigations on Structural Stability, Elastic Properties and Electronic Structure of Mg32 (Al, Zn) 49 Phase and MgZn2 Phase, Crystals 12(5) (2022) 683.
[46] J.-M. Joubert, Crystal chemistry and Calphad modeling of the σ phase, Progress in Materials Science 53(3) (2008) 528-583.
[47] F.C. Frank, J.S. Kasper, Complex alloy structures regarded as sphere packings. I. Definitions and basic principles, Acta Crystallographica 11(3) (1958) 184-190.